Formation of Alkali Metal/Alkaline Earth Cation Water Clusters, $M(H_2O)_{1-6}$, M = Li^+, Na^+, K^+, Mg^{2+}, and Ca^{2+}: An Effective Fragment Potential (EFP) Case Study

Grant N. Merrill,* Simon P. Webb, and Donald B. Bivin

*Department of Computational Chemistry, Covalent Partners, LLC, 330 Beach Road,
Burlingame, California 94010*

Received: September 6, 2002; In Final Form: October 30, 2002

To assess the ability of the effective fragment potential (EFP) method to describe the hydration of simple cations, calculations have been carried out on alkali metal (Li^+, Na^+, and K^+)/alkaline earth (Mg^{2+} and Ca^{2+}) cation water clusters containing up to six water molecules. The restricted Hartree−Fock (RHF) and second-order Møller−Plesset (MP2) perturbation methods have also been employed in the study. It is shown that the EFP method is capable of accurately reproducing RHF differential standard enthalpies of hydration for the alkali metal and calcium cation water systems. The EFP method also reproduces experimental differential and total standard enthalpies of hydration for the alkali metal cation water complexes. Good agreement is also found among the EFP and ab initio levels of theory for the enthalpies of the calcium cation water clusters. Possible reasons for discrepancies between the EFP results and those obtained at the ab initio levels for the structures of the $Na^+(H_2O)_{1-6}$ and $Mg^{2+}(H_2O)_{1-6}$ clusters and the energetics of the $Mg^{2+}(H_2O)_{1-6}$ clusters are discussed. A model chemistry is suggested that is based upon EFP/6-31+G* optimizations and Hessians and single-point energies at the MP2/aug-cc-pVDZ level of theory (i.e., MP2/aug-cc-pVDZ//EFP/6-31+G*).

I. Introduction

The importance of understanding and accurately describing solvation cannot be overemphasized, given that most chemistry occurs in the condensed phase. The accurate description of solvation phenomena continues, however, to present a significant challenge to theoretical chemistry. The modeling of aqueous systems in particular poses a unique set of problems owing to the polar and protic nature of the solvent. For example, because of water's ability to participate as both a hydrogen bond donor and acceptor, the solvation of cationic and anionic systems is accomplished by very different means.

The alkali metal and alkaline earth cations play many important roles in nature. For instance, they serve as counterions, maintain concentration gradients, and are essential elements of enzymatic processes in biological systems.[1] Such systems cannot be understood without taking into account the cation−water interactions. To cite but a single example from the literature, Feller[2] has shown that the preferential binding of K^+ to 18-crown-6 ether occurs only in the presence of water.

Continuum approaches[3] to the problem of solvation treat the solvent in bulk as a polarizable medium. They have enjoyed a great deal of popularity among computational chemists because of their relative simplicity, which in turn makes them amenable to large chemical systems. It is becoming increasingly clear, however, that even the most sophisticated of these models (e.g., the polarizable continuum model, PCM[4]) often obscure much of the underlying physics of solute−solvent and solvent−solvent interactions, and it is these discrete interactions that often give rise to the complex and subtle solvation behavior seen in aqueous systems.

As a result of the inherent limitations of continuum methods, various approaches that offer a molecular representation of the solvent have been developed. One such method is the so-called supermolecular approach,[5] where explicit solvent molecules are added and treated at the same level of theory as that used for the solute. However, this supermolecular approach does come with a substantial increase in computational expense. For example, at the ab initio level of theory, the solvent molecules must be described with a wavefunction, and the attendant cost increases rapidly with the number of basis functions and the level of theory. Each solvent molecule also adds $3N$ degrees of freedom, where N is the number of atoms in the solvent molecule. This in turn complicates the sampling of the configurational space (e.g., optimizations or trajectories). Even with increasingly powerful computer hardware and efficient algorithms, these supermolecular treatments have been limited to a handful of solvent molecules at ab initio levels of theory.

In an attempt to defray the cost of ab initio supermolecular methods, while at the same time retaining their accuracy, a number of semiclassical techniques[6] have been advanced. These approaches construct the Hamiltonian in terms of both quantum mechanical and classical operators. One of the more promising of these approaches is due to Stevens, Gordon, and co-workers[7] and is known as the effective fragment potential (EFP) method, a full description of which may be found in the literature. Briefly, the system of interest is partitioned into quantum mechanical and classical regions. The quantum mechanical region, also referred to as the "active" region, includes those parts of the system requiring a wavefunction description owing to the occurrence of quantum events (e.g., the formation or lysis of bonds). The classical or "spectator" region contains those elements that exert an influence on, but are not directly involved in, phenomena associated with the active region (e.g., a charge distribution). The interactions between these two regions and within the classical region are governed by three one-electron terms in the Hamiltonian corresponding to electrostatic (ES), polarization (POL), and charge transfer (CT)/exchange repulsion

---

* Corresponding author. E-mail: grantm@covalent.to. Phone: (650) 227-7736. Fax: (650) 227-7701.

10.1021/jp0220128 CCC: $25.00

(EX) effects. The electrostatic component is implemented via a series of multipole expansions located at the nuclei and bond midpoints. These expansions are carried out through the octupole term. Polarizable dipole tensors situated at the centroids of charge for all localized valence orbitals are employed in the treatment of polarization. These induced dipoles are allowed to interact with the electric field of the active region and are iterated to self-consistency. Effects arising from charge transfer and exchange repulsion are handled through a series of Gaussian potential functions located at the nuclei. In the case of the current effective fragment potential for the water molecule, these functions are fit to the residual energy for a series of water dimer conformations from which the electrostatic and polarization components have been subtracted. As the most computationally demanding step in any ab initio calculation involves the two-electron integrals, solvent-related integrals contribute negligibly to the overall expense of the computation. It is important to note that the present implementation of the effective fragment potential makes use of the rigid body approximation. Bond formation or lysis involving the effective fragment potentials is, therefore, not possible. Similarly, explicit charge transfer to or from the effective fragment potential is not permitted.

It is important to appreciate fully the computational savings involved by making use of semiclassical methods. In the EFP method, only a subset of the atoms in the system is described by a wavefunction, reducing the number of basis functions required. In all of the EFP calculations reported below, the quantum mechanical part of the computation (corresponding to the active region) includes only the cation; all water molecules are treated with effective fragment potentials. This fact serves to reduce drastically the cost of the computation. As an example, consider the largest systems studied in the present work, $K^+(H_2O)_6$ and $Ca^{2+}(H_2O)_6$. Even with a rather modest basis set (e.g., 6-31+G*), 168 basis functions contribute to the wavefunction in the all ab initio approach. In contrast, the EFP approach uses only 30 basis function. This reduces the cost of the EFP computation to less than 0.1% of the complete quantum mechanical description.[8] This difference is even more dramatic for post Hartree–Fock (HF) methods (e.g., MP2), which scale even less favorably with the number of basis functions.[9]

Since the introduction of the method, an increasing number of EFP studies[10] have appeared in the literature. The method has proved successful at reproducing both experimental and ab initio results. Most of these studies have, however, involved neutral systems (notable exceptions being the work of Webb and Gordon,[10d] Gordon and Petersen,[10e] and Damrauer[10g]), and questions remain regarding the method's ability to treat charged systems. It is for this reason that the current study was undertaken.

This paper describes an investigation of hydrated alkali metal (Li^+, Na^+, and K^+) and alkaline earth (Mg^{2+} and Ca^{2+}) cations, which are all, with the possible exception of Li^+, of biological importance. An examination of the literature reveals that these systems have been the focus of numerous experimental[11] and theoretical[12] studies. Both the differential (eq 1) and total (eq 2) standard enthalpies of hydration by up to six water molecules were determined in the current study,

$$M(H_2O)_{n-1} + H_2O \rightarrow M(H_2O)_n \tag{1}$$

$$M + nH_2O \rightarrow M(H_2O)_n \tag{2}$$

where $n = 1-6$ and $M = Li^+, Na^+, K^+, Mg^{2+}$, and Ca^{2+}. These calculations were performed to assess the EFP method's ability to reproduce ab initio and experimental results for the cationic systems. As has been observed in the experimental literature,[11g,k] charge-transfer processes are potentially important reaction pathways for small divalent cationic clusters. This is particularly true for metals whose second ionization potentials (IP) lie below those of the first IP of the clustering solvent. In the current context, these processes are most relevant for the $Mg^{2+}(H_2O)_{1-6}$ clusters ($IP(Mg^+) = 15.0$ eV; $IP(H_2O) = 12.6$ eV). As such, electron (eq 3) and proton (eq 4) transfer have been shown to be competitive with evaporation (the reverse reaction of eq 1).

$$Mg^{2+}(H_2O)_n \rightarrow Mg^+(H_2O)_{n-1} + H_2O^+ \tag{3}$$

$$Mg^{2+}(H_2O)_n \rightarrow M(H_2O)_{n-m-2} + H_3O^+(H_2O)_m \tag{4}$$

Whereas these processes are important in and of themselves, they are beyond the focus of the current study. Moreover, the EFP method is incapable of modeling such reactions (vide supra). Ab initio water molecules would need to be included in the active region, and open-shell wavefunctions would be required.

Along with a study on anionic systems,[13] the present study will complete a comprehensive survey of the EFP method's performance in describing hydrated neutral, zwitterionic, and charged systems.

II. Methods

The initial implementation of the effective fragment potential (EFP) method was designed to reproduce results obtained at the Hartree–Fock (HF) level of theory with a double split-valence polarized basis set. Restricted Hartree–Fock (RHF) calculations were therefore carried out for comparison. A double split-valence basis set, to which sets of polarization (six d orbitals) and diffuse (sp orbitals) functions were added to all nonhydrogenic atoms, was selected and will be referred to as 6-31+G*.[14] This permits a direct comparison between the EFP and RHF results. As the EFP and RHF methods do not account for electron correlation, frozen core second-order Møller–Plesset (MP2) perturbation theory[15] was employed in conjunction with the 6-31+G* basis set. No orbitals were frozen for the hydrogen and lithium atoms whereas the 1s orbitals were frozen for the oxygen, sodium, and magnesium atoms. The 1s, 2s, and 2p orbitals were frozen for the potassium and calcium atoms. In the EFP calculations, only the cations are treated with ab initio wavefunctions.

All structures were fully optimized at the above levels of theory so that the root-mean-square gradient and the largest component of the gradient were less than 0.012 and 0.004 kcal/mol Å, respectively. To verify that the stationary points on the potential energy surfaces were minima, Hessian matrices were also calculated. Analytic Hessians were computed at the RHF level of theory whereas double-differenced numerical Hessians were determined at the EFP and MP2 levels. The Hessian matrices permitted zero-point energies (ZPE) and finite temperature (FT) corrections to 298.15 K and 1 atm (H^0) to be calculated. Empirical scaling factors of 0.90, 0.90, and 0.94 were applied to the EFP, RHF, and MP2 frequencies, respectively.[16]

Additional benchmark calculations were performed upon the Na^+ and Mg^{2+} clusters at the MP2 level with the aug-cc-pVDZ and aug-cc-pVTZ correlation consistent basis sets of Dunning.[17] Here, no diffuse (aug) functions were added to the metal cations. The structures were fully optimized, their associated Hessian matrices were determined with the aug-cc-pVDZ basis set, and single-point energy calculations were carried out with the aug-cc-pVTZ basis set upon the optimized geometries (i.e., MP2/aug-cc-pVTZ//MP2/aug-cc-pVDZ).

Unless otherwise specified, all energies are in kcal/mol and correspond to enthalpies at 298.15 K and 1 atm; all distances are in Å. All of the calculations were carried out with the GAMESS program,[18] which is freely available at www.msg.ameslab.gov.

III. Results and Discussion

The cation/water cluster structures selected for study were based upon the earlier results of Glendening and Feller.[12h,i] Those structures previously determined to have the lowest enthalpies of hydration served as starting points for full optimizations at the above levels of theory. A detailed comparison between the results of Glendening and Feller and ours can be found in the notes after refs 12h (alkali metal cation systems) and 12i (alkaline earth cation systems). It is clear that as cluster size and temperature increase so does the importance of entropic effects. Given the small size of the clusters ($n \leq 6$) and moderate temperature (T = 298.15 K), the enthalpic contribution to the free energy is predicted to dominate that of the entropy. Enthalpies, and not free energies, are therefore reported in the current study. Experimental enthalpies are moreover available for the current systems.

A. Alkali Metal Systems $M^+(H_2O)_{1-6}$, M = Li, Na, and K. Table 1 lists the computed distances between the alkali metal cation (M^+) and the oxygen atom (O) of the water molecule in units of angstroms for the alkali metal cation/water clusters, $M^+(H_2O)_{1-6}$, where M = Li, Na, and K. Figure 1 presents illustrations of the corresponding structures. As no experimental structural data is available, all comparisons were made vis-à-vis the restricted Hartree−Fock (RHF) structures. These particular comparisons were made because the effective fragment potential (EFP) method was developed to reproduce HF results.

In the alkali metal systems, the water molecules in the first solvation shell have their dipoles radially directed toward the central cation. They tend to array themselves in a highly symmetric fashion so as to minimize repulsive interactions between one another. This packing allows up to four water molecules in the first solvation shell. The fifth and sixth water molecules contribute to the second solvation shell (see structures VB and VIB in Figure 1). Here again, they align their dipoles toward the central cation, but they deviate slightly from collinearity so as to permit hydrogen bonding with water molecules in the first solvation shell. Each solvation shell possesses a characteristic cation−oxygen atom distance that is a function of the specific cation.

The structures found using the EFP method are in good agreement with those determined at the RHF/6-31+G* level of theory for the Li^+ and K^+ clusters. The EFP calculations slightly lengthen the $M^+\cdots O$ distances, leading to mean unsigned errors, MUE, of only 0.04 and 0.01 Å for the first solvation shells of the $Li^+(H_2O)_{1-6}$ and $K^+(H_2O)_{1-6}$ clusters, respectively. The differences are only slightly greater for the second solvation shell: $Li^+(H_2O)_{1-6}$, MUE = 0.02 Å and $K^+(H_2O)_{1-6}$, MUE = 0.06 Å. The agreement between the EFP and RHF calculations for the sodium clusters is not as impressive. The MUEs for the first and second solvation shells are 0.15 and 0.18 Å, respectively. This lengthening of the $M^+\cdots O$ bonds parallels that found for EFP anion/water complexes.[13] As will be shown (vide infra), similar disparities are also found for the magnesium clusters. The MP2 method exhibits its characteristic shortening of noncovalent bonds. Whereas the agreement between the MP2 and RHF results for the first solvation shell is fairly good, it worsens for the second solvation shell. Clearly, electron correlation has its greatest impact on the weaker solvent−solvent interactions in which dispersion effects are far more important.

For the $Na^+(H_2O)_{1-6}$ clusters, an additional series of MP2 optimizations was carried out. As correlated methods are particularly sensitive to basis set, often requiring larger numbers of high angular momentum functions to recover a significant percentage of electron correlation, the augmented, correlation-consistent, double split-valence polarized basis set (aug-cc-pVDZ) of Dunning[17] was used in these optimizations. The 1s orbitals of the oxygen and sodium atoms were again frozen. These results are presented in Table 1. An examination of the data reveals that little difference accrues from this expanded basis set; the RHF/6-31+G*, MP2/6-31+G*, and MP2/aug-cc-pVDZ structures are essentially identical. This suggests that the RHF/6-31+G* level of theory gives reasonable geometries.

Finally, it is worth noting the very small standard deviations (σ) found for the alkali metal cation/water clusters at all levels of theory. The differences also appear to be quite systematic as evinced by the fact that the magnitudes of the mean signed errors, MSE, are often equal to those of the mean unsigned errors (i.e., |MSE| = MUE).

Table 2 lists the experimental and computed differential enthalpies of hydration at 298.15 K and 1 atm ($\Delta\Delta_r H^0$) (i.e., the standard enthalpies for the addition of a single water molecule to a cluster of a given size (eq 1)). A comparison of the values obtained at the EFP/6-31+G* and RHF/6-31+G* levels shows excellent agreement between the two for the alkali metal clusters. This clearly demonstrates that the EFP method is capable of reproducing RHF results for charged systems. Ultimately, any method's usefulness depends on its ability to reproduce experimental results. Table 2 shows that the RHF/6-31+G* level of theory gives values for $\Delta\Delta_r H^0$ that are usually within experimental accuracy, ±1.0 to 2.0 kcal/mol.[19] As the EFP method so successfully reproduces the RHF results in these cases, it too is in good agreement with experiment. The MP2/6-31+G* level shows a slight increase in the binding energies, and whereas the agreement with experiment is still good, it is not as good as for the EFP/6-31+G* and RHF/6-31+G* levels. Benchmark MP2 calculations on the $Na^+(H_2O)_{1-6}$ clusters with the aug-cc-pVDZ and aug-cc-pVTZ bases suggest that this is a basis set effect (i.e., with the larger basis set, the MP2 level is also in excellent agreement with experiment).

As it is often desirable to know the total standard enthalpies of hydration ($\Delta_r H^0$), Table 3 lists these experimental and calculated values as well. For the $Li^+(H_2O)_{1-6}$ clusters, the EFP/6-31+G* total enthalpies are in quite close agreement with those obtained at the RHF/6-31+G* level. Compared to experiment, both of these levels of theory give somewhat overbound clusters (EFP: MSE = −4.7 kcal/mol; RHF: MSE = −6.8 kcal/mol). The MP2/6-31+G* level predicts even more overbinding (MSE = −13.1 kcal/mol). For the $Na^+(H_2O)_{1-6}$ clusters, the EFP $\Delta_r H^0$ values show consistently weaker binding than that found at the RHF/6-31+G* level. Compared to experiment, the RHF/6-31+G* and MP2/6-31+G* levels of theory again show overbinding (RHF: MUE = 5.7 kcal/mol; MP2: MUE = 11.2 kcal/mol). Consequently, the EFP/6-31+G* values are found to compare more favorably with experiment than the ab initio calculations. For the $K^+(H_2O)_{1-6}$ clusters, the EFP/6-31+G* total enthalpies are in very close agreement with those found at the RHF/6-31+G* level. Furthermore, the EFP/6-31+G* and RHF/6-31+G* total enthalpies are in excellent agreement with experiment (EFP: MUE = 1.0 kcal/mol; RHF: MUE = 0.4

TABLE 1: Comparison of Computed Geometries for Alkali Metal/Alkaline Earth Cation Water Clusters (Å)[a]

$Li^+(H_2O)_n$		RHF/6-31+G*		EFP/6-31+G*				MP2/6-31+G*				MP2/aug-cc-pVDZ			
n	cmpd	first	second	first	Δ	second	Δ	first	Δ	second	Δ	first	Δ	second	Δ
1	I	1.85		1.88[b]	0.03			1.85	0.00						
2	IIA	1.88		1.92	0.04			1.86	−0.02						
3	III	1.92		1.96	0.04			1.89	−0.03						
4	IV	1.97		2.00	0.03			1.92[c]	−0.05						
5	VB	1.96	3.83	2.00	0.04	3.80	−0.03	1.92[d]	−0.04	3.71	−0.12				
6	VIB	1.97	3.88	2.00	0.03	3.88	0.00	1.95[e]	−0.05	3.71	−0.17				
mean					0.04		−0.02		−0.03		−0.14				
standard deviation					0.01		0.02		0.02		0.04				

$Na^+(H_2O)_n$		RHF/6-31+G*		EFP/6-31+G*				MP2/6-31+G*				MP2/aug-cc-pVDZ			
n	cmpd	first	second	first	Δ	second	Δ	first	Δ	second	Δ	first	Δ	second	Δ
1	I	2.23		2.39	0.16			2.25	0.02			2.21	−0.02		
2	IIB	2.25		2.40	0.15			2.26	0.01			2.24	−0.01		
3	III	2.28		2.43	0.15			2.28	0.00			2.27[f]	−0.01		
4	IV	2.31		2.46	0.15			2.29	−0.02			2.30[g]	−0.01		
5	VB	2.30	4.12	2.45	0.15	4.30	0.18	2.28	−0.02	4.04	−0.08	2.30[h]	0.00	4.05	−0.07
6	VIB	2.30	4.16	2.45	0.15	4.33	0.17	2.28	−0.02	4.10	−0.06	2.30[i]	0.00	4.10	−0.06
mean					0.15		0.18		0.00		−0.07		−0.01		−0.07
standard deviation					0.00		0.01		0.02		0.01		0.01		0.01

$K^+(H_2O)_n$		RHF/6-31+G*		EFP/6-31+G*				MP2/6-31+G*				MP2/aug-cc-pVDZ			
n	cmpd	first	second	first	Δ	second	Δ	first	Δ	second	Δ	first	Δ	second	Δ
1	I	2.65		2.66	0.01			2.60	−0.05						
2	IIB	2.68		2.69	0.01			2.63[j]	−0.05						
3	III	2.71		2.72	0.01			2.66	−0.05						
4	IV	2.74		2.75	0.01			2.68	−0.06						
5	VB	2.73	4.52	2.74	0.01	4.58	0.06	2.76[k]	−0.06	4.43	−0.09				
6	VIB	2.72	4.55	2.73	0.01	4.60	0.05	2.66	−0.06	4.46	−0.09				
mean					0.01		0.06		−0.06		−0.09				
standard deviation					0.00		0.01		0.01		0.00				

$Mg^{2+}(H_2O)_n$		RHF/6-31+G*		EFP/6-31+G*				MP2/6-31+G*				MP2/aug-cc-pVDZ			
n	cmpd	first	second	first	Δ	second	Δ	first	Δ	second	Δ	first	Δ	second	Δ
1	I	1.94		2.10	0.16			1.95	0.01			1.94	0.00		
2	IIA	1.96		2.12	0.16			1.97	0.01			1.96	0.00		
3	III	1.98		2.14	0.16			1.99	0.01			1.98	0.00		
4	IV	2.01		2.17	0.16			2.02	0.01			2.01	0.00		
5	VA	2.07		2.20	0.13			2.07	0.00			2.06[l]	−0.01		
6	VIA	2.11		2.22	0.11			2.10	−0.01			2.09[m]	−0.02		
mean					0.15				0.00				0.00		
standard deviation					0.02				0.01				0.01		

$Ca^{2+}(H_2O)_n$		RHF/6-31+G*		EFP/6-31+G*				MP2/6-31+G*				MP2/aug-cc-pVDZ			
n	cmpd	first	second	first	Δ	second	Δ	first	Δ	second	Δ	first	Δ	second	Δ
1	I	2.29		2.34	0.05			2.27	−0.02						
2	IIB	2.32		2.36	0.04			2.30	−0.02						
3	III	2.35		2.39	0.04			2.33	−0.02						
4	IV	2.37		2.41	0.04			2.35	−0.02						
5	VA	2.40		2.44	0.04			2.38	−0.02						
6	VIA	2.43		2.47	0.04			2.39	−0.04						
mean					0.04				−0.02						
standard deviation					0.00				0.01						

[a] Values are average distances between the cation and the oxygen atoms of water molecules in the first and second solvation shells. Differences (Δ) are relative to the RHF/6-31+G* level of theory. See Figure 1 for structures. [b] All EFP structures formally have C_1 symmetry. This structure has C_s-like symmetry. The C_{2v}-like structure is a transition state (175i cm^{-1}). [c–m] The MP2 vibrational analyses were performed numerically via double differencing. A number of clusters exhibited small imaginary frequencies that are probably numerical artifacts. These imaginary frequencies are (c) 25i and 25i cm^{-1}, (d) 9i cm^{-1}, (e) 66i cm^{-1}, (f) 17i cm^{-1}, (g) 128i, 102i, 76i, 76i, and 32i cm^{-1}, (h) 55i, 46i, and 29i cm^{-1}, (i) 58i cm^{-1}, (j) 14i cm^{-1},[1] (k) 3i cm^{-1}, (l) 86i cm^{-1}, and (m) 240i, 240i, and 224i cm^{-1}.

kcal/mol). Once again, the MP2/6-31+G* level of theory shows overbinding with respect to experiment (MUE = 6.5 kcal/mol). The RHF/6-31+G* and MP2/6-31+G* levels of theory clearly predict total enthalpies of hydration for the $Li^+(H_2O)_{1-6}$ and $Na^+(H_2O)_{1-6}$ clusters that are considerably worse than for those of the corresponding differential enthalpies of hydration. Solely on the basis of comparison with experiment, the EFP/6-31+G* total enthalpies are superior to those found using a higher level of theory, MP2/6-31+G*. In fact, all of the MP2/6-31+G* results are quite poor, even for the $K^+(H_2O)_{1-6}$ clusters. An examination of the benchmark MP2/aug-cc-pVDZ and MP2/aug-cc-pVTZ//MP2/aug-cc-pVDZ calculations on the $Na^+(H_2O)_{1-6}$ clusters reveals that an increase in the quality of the basis set has a quite dramatic effect upon the total enthalpies

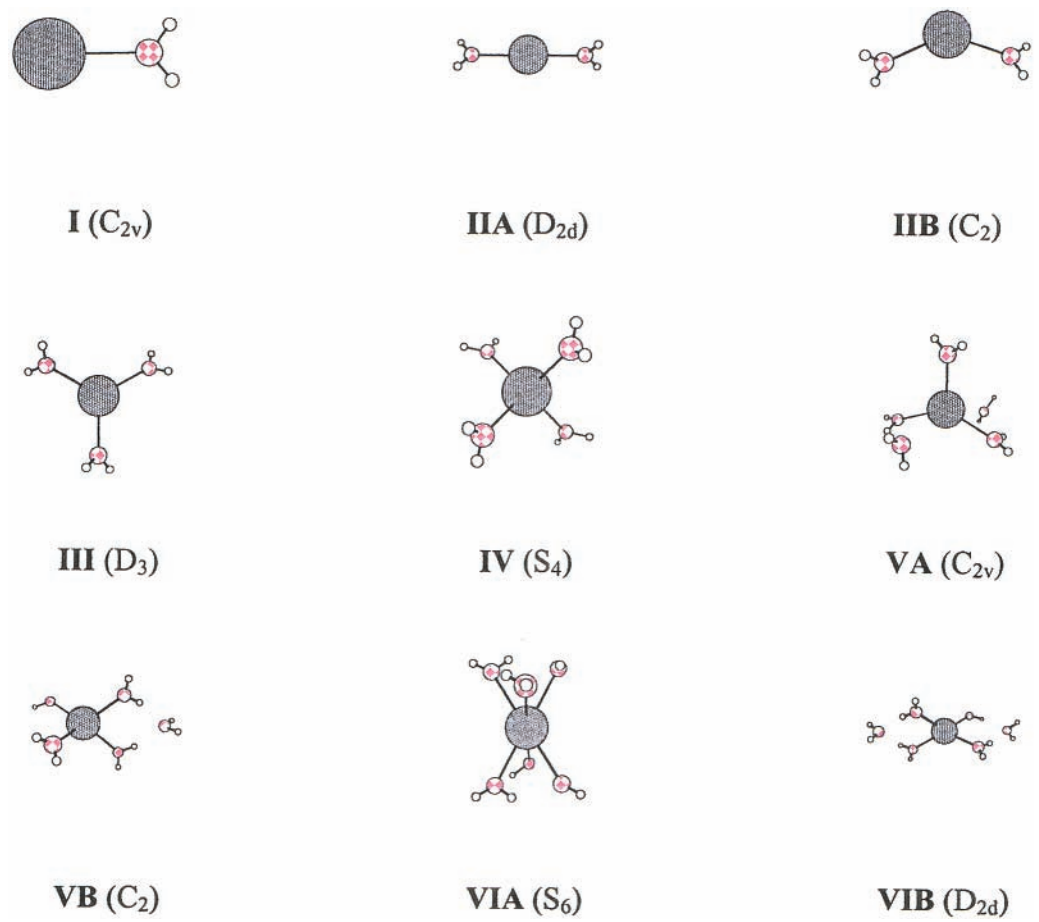

Figure 1. Schematic representation of alkali metal/alkaline earth cation water clusters. See Table 1 for average bond distances between the cation and oxygen atoms of the water molecules.

of hydration. This, together with the good performance of the EFP method, suggests the presence of basis set superposition errors (BSSE) in these clusters. (It should be recalled that EFP water molecules have no basis functions that could introduce such an error.) In fact, it has been noted in the literature[20] that the use of incomplete basis sets can lead to significant BSSE in the current cationic systems.

A reduced variational space (RVS)[21] analysis was performed at the RHF/6-31+G* level of theory (Table 4) to permit the extent of BSSE to be assessed as well as to allow for the total interaction energy to be decomposed into electrostatic and exchange (ESEX), polarization (POL), and charge-transfer (CT) components. The BSSE was found to average 1.1 kcal/mol per water molecule for the $Li^+(H_2O)_{1-6}$ clusters. When a counterpoise (CP) correction[22] was applied to the clustering reactions, the average error dropped from −6.8 to −2.8 kcal/mol whereas the standard deviation went from 2.6 to 2.0 kcal/mol. These results are all the more interesting when viewed in light of the EFP calculations. As previously mentioned, the EFP water molecules do not possess any basis functions, and a basis set superposition error cannot result. The EFP method leads, therefore, to low overall errors for the alkali metal cation/water clusters. The CP-corrected total enthalpies for the $Na^+(H_2O)_{1-6}$ clusters improve more modestly: mean, −5.7 to −3.1 kcal/mol; σ, 2.4 to 1.3 kcal/mol. This is due to a smaller average BSSE per water molecule (0.7 kcal/mol). The CP correction actually leads to poorer agreement with experiment for the $K^+(H_2O)_{1-6}$ clusters: mean, 0.2 to 1.4 kcal/mol; σ, 0.4 to 0.9 kcal/mol. Here, the average BSSE per water molecule is only 0.3 kcal/mol.

Table 4 also contains the Mulliken charges[23] on the metals, q(M), and average bond orders between the metal cations and oxygen atoms of the water molecules, BO(M···O) at the RHF/6-31+G* level. For the $Li^+(H_2O)_{1-6}$ clusters, appreciable charge has been transferred from the water molecules to the metal cations. (See also the charge transferred per water molecule, $q(H_2O)$, in Table 4.) For example, 0.32 e^- have been transferred to Li^+ in the $Li^+(H_2O)_6$ cluster. This leads to the formation of dative-type bonds in these systems. Essentially no charge transfer is seen for the Na^+ and K^+ clusters. As the results at the EFP level are in excellent agreement with the RHF/6-31+G* calculations, it is clear that the effect of charge transfer of up to 0.13 e^- per water molecule is easily described by the model.

To assess the importance of both the zero-point energy (ZPE) and finite temperature (FT) corrections, the differential and total internal energies and enthalpies at 0 K and 1 atm were also computed. The mean signed errors and standard deviations can be found in Table 5. The total internal energies ($\Delta_r E^0$) are far worse than the total enthalpies ($\Delta_r H^0$). The enthalpies at 0 and 298.15 K are quite similar. One is led to conclude that, whereas the zero-point energies are important, the value of the finite temperature corrections is less obvious. Similar trends are seen for the differential internal energies ($\Delta\Delta_r E^0$) and enthalpies ($\Delta\Delta_r H^0$) at 0 K. It should be noted, however, that the differences here are far less pronounced: all levels of theory reproduce the experimental differential enthalpies of hydration reasonably well. For the purposes of comparison to experimental total enthalpies, zero-point energies are absolutely essential. Zero-point energies

TABLE 2: Differential Standard Enthalpies, $\Delta\Delta_rH^0$, of Hydration for the Formation of Alkali Metal/Alkaline Earth Cation Water Clusters ($X(H_2O)_{n-1} + H_2O \rightarrow X(H_2O)_n$, X = Li^+, Na^+, K^+, Mg^{2+}, and Ca^{2+}, n = 1−6) (kcal/mol)[a]

	exptl[b]	EFP/6-31+G*		RHF/6-31+G*		MP2/6-31+G*		MP2/aug-cc-pVDZ		MP2/aug-cc-pVTZ	
$Li^+(H_2O)_n$	$\Delta\Delta_rH^0$	$\Delta\Delta_rH^0$	error	$\Delta\Delta_rH^0$	error	$\Delta\Delta_rH^0$	error	$\Delta\Delta_rH^0$	error	$\Delta\Delta_rH^0$	error
1	−34.0	−34.9	−0.9	−35.8	−1.8	−36.3	−2.3				
2	−25.8	−29.7	−3.9	−30.7	−4.9	−32.3	−6.5				
3	−20.7	−22.5	−1.8	−23.0	−2.3	−24.6	−3.9				
4	−16.4	−16.7	−0.3	−16.2	0.2	−20.2	−3.8				
5	−13.9	−12.0	1.9	−12.3	1.6	−15.2	−1.3				
6	−12.1	−10.9	1.2	−11.5	0.6	−14.7	−2.6				
mean			−0.6		−1.1		−3.4				
std dev			2.1		2.4		1.8				

	exptl[b]	EFP/6-31+G*		RHF/6-31+G*		MP2/6-31+G*		MP2/aug-cc-pVDZ		MP2/aug-cc-pVTZ	
$Na^+(H_2O)_n$	$\Delta\Delta_rH^0$	$\Delta\Delta_rH^0$	error	$\Delta\Delta_rH^0$	error	$\Delta\Delta_rH^0$	error	$\Delta\Delta_rH^0$	error	$\Delta\Delta_rH^0$	error
1	−24.0	−23.1	0.9	−25.5	−1.5	−26.1	−2.1	−23.0	1.0	−23.9	0.1
2	−19.8	−20.3	−0.5	−22.3	−2.5	−23.4	−3.6	−19.8	0.0	−22.3	−2.5
3	−15.8	−17.1	−1.3	−18.4	−2.6	−19.4	−3.6	−17.4	−1.6	−16.6	−0.8
4	−13.8	−14.0	−0.2	−14.8	−1.0	−17.2	−3.4	−17.5	−3.7	−17.9	−4.1
5	−12.3	−11.4	0.9	−11.7	0.6	−15.7	−3.4	−13.0	−0.7	−13.3	−1.0
6	−10.7	−11.2	−0.5	−11.4	−0.7	−16.1	−5.4	−10.2	0.5	−11.1	−0.4
mean			−0.1		−1.3		−3.6		−0.8		−1.4
std dev			0.9		1.2		1.1		1.7		1.4

	exptl[c]	EFP/6-31+G*		RHF/6-31+G*		MP2/6-31+G*		MP2/aug-cc-pVDZ		MP2/aug-cc-pVTZ	
$K^+(H_2O)_n$	$\Delta\Delta_rH^0$	$\Delta\Delta_rH^0$	error	$\Delta\Delta_rH^0$	error	$\Delta\Delta_rH^0$	error	$\Delta\Delta_rH^0$	error	$\Delta\Delta_rH^0$	error
1	−17.9	−18.6	−0.7	−18.3	−0.4	−20.1	−2.2				
2	−16.1	−15.7	0.4	−15.3	0.8	−17.5	−1.4				
3	−13.2	−13.8	−0.6	−13.4	−0.2	−14.3	−1.1				
4	−11.8	−11.6	0.2	−11.2	0.6	−12.7	−0.9				
5	−10.7	−11.1	−0.4	−11.0	−0.3	−15.0	−4.3				
6	−10.0	−10.9	−0.9	−10.8	−0.8	−13.5	−3.5				
mean			−0.3		0.0		−2.2				
std dev			0.5		0.6		1.4				

	exptl[d]	EFP/6-31+G*		RHF/6-31+G*		MP2/6-31+G*		MP2/aug-cc-pVDZ		MP2/aug-cc-pVTZ	
$Mg^{2+}(H_2O)_n$	$\Delta\Delta_rH^0$	$\Delta\Delta_rH^0$	error	$\Delta\Delta_rH^0$	error	$\Delta\Delta_rH^0$	error	$\Delta\Delta_rH^0$	error	$\Delta\Delta_rH^0$	error
1		−66.6		−80.1		−81.6		−77.5		−80.5	
2		−60.8		−71.2		−72.7		−68.5		−74.4	
3		−52.6		−58.4		−60.2		−56.1		−56.4	
4		−44.8		−47.2		−49.9		−46.5		−47.8	
5	−26.3	−35.3	−9.0	−31.3	−5.0	−34.9	−8.6	−33.7	−7.4	−39.1	−12.8
6	−24.2	−28.9	−4.7	−28.8	−4.6	−32.5	−8.3	−31.7	−7.5	−43.5	−19.3
mean											
std dev											

	exptl[d]	EFP/6-31+G*		RHF/6-31+G*		MP2/6-31+G*		MP2/aug-cc-pVDZ		MP2/aug-cc-pVTZ	
$Ca^{2+}(H_2O)_n$	$\Delta\Delta_rH^0$	$\Delta\Delta_rH^0$	error	$\Delta\Delta_rH^0$	error	$\Delta\Delta_rH^0$	error	$\Delta\Delta_rH^0$	error	$\Delta\Delta_rH^0$	error
1		−52.6		−55.0		−58.0					
2		−46.9		−48.1		−51.2					
3		−42.4		−43.1		−44.7					
4		−37.4		−37.5		−39.8					
5	−26.7	−30.9	−4.2	−30.1	−3.4	−32.9	−6.2				
6	−22.0	−27.9	−5.9	−27.2	−5.2	−30.6	−8.6				
mean											
std dev											

[a] MP2/aug-cc-pVTZ values are single-point energies on MP2/aug-cc-pVDZ geometries. See the text for details. [b] Reference 11b. [c] Reference 11a. [d] Reference 11j.

also lead to improved agreement with experimental differential enthalpies.

B. Alkaline Earth Systems $M^{2+}(H_2O)_{1-6}$, M = Mg and Ca. Analogous calculations were also carried out on the alkaline earth cation/water clusters, $Mg^{2+}(H_2O)_{1-6}$ and $Ca^{2+}(H_2O)_{1-6}$. Table 1 offers a comparison of the cluster structures whereas Tables 2 and 3 list the computed differential ($\Delta\Delta_rH^0$) and total (Δ_rH^0) standard enthalpies of hydration, respectively. Unfortunately, experimental enthalpies are available only for the magnesium and calcium cation water clusters with five and six water molecules.

As noted in the previous section, the EFP/6-31+G* optimizations predict significantly longer $Mg^{2+}\cdots O$ bond distances (MSE = 0.15 Å; σ = 0.02 Å) than found at the RHF/6-31+G* level of theory. For the calcium cation clusters, the $Ca^{2+}\cdots O$ distances at the EFP/6-31+G* level agree much more closely with those predicted at the RHF/6-31+G* level (MSE = MUE = 0.04 Å; σ = 0.00 Å). The MP2/6-31+G* level essentially reproduces

TABLE 3: Total Standard Enthalpies, $\Delta_r H^0$, of Hydration for the Formation of Alkali Metal/Alkaline Earth Cation Water Clusters ($X + nH_2O \rightarrow X(H_2O)_n$, X = Li^+, Na^+, K^+, Mg^{2+}, and Ca^{2+}, $n = 1-6$) in kcal/mol[a]

	exptl[b]	EFP/6-31+G*		RHF/6-31+G*		MP2/6-31+G*		MP2/aug-cc-pVDZ		MP2/aug-cc-pVTZ	
$Li^+(H_2O)_n$	$\Delta_r H^0$	$\Delta_r H^0$	error	$\Delta_r H^0$	error	$\Delta_r H^0$	error	$\Delta_r H^0$	error	$\Delta_r H^0$	error
1	−34.0	−34.9	−0.9	−35.8	−1.8	−36.3	−2.3				
2	−59.8	−64.9	−4.8	−66.6	−6.8	−68.6	−8.8				
3	−80.5	−87.1	−6.6	−89.6	−9.1	−93.2	−12.7				
4	−96.9	−103.8	−6.9	−105.8	−8.9	−113.4	−16.5				
5	−110.8	−115.8	−5.0	−118.1	−7.3	−128.6	−17.8				
6	−122.9	−126.7	−3.8	−129.6	−6.7	−143.3	−20.4				
mean			−4.7		−6.8		−13.1				
std dev			2.2		2.6		6.7				

	exptl[b]	EFP/6-31+G*		RHF/6-31+G*		MP2/6-31+G*		MP2/aug-cc-pVDZ		MP2/aug-cc-pVTZ	
$Na^+(H_2O)_n$	$\Delta_r H^0$	$\Delta_r H^0$	error	$\Delta_r H^0$	error	$\Delta_r H^0$	error	$\Delta_r H^0$	error	$\Delta_r H^0$	error
1	−24.0	−23.1	0.9	−25.5	−1.5	−26.1	−2.1	−23.0	1.0	−23.9	0.1
2	−43.8	−43.4	0.4	−47.8	−4.0	−49.4	−5.6	−42.8	1.0	−46.2	−2.4
3	−59.6	−60.5	−0.9	−66.2	−6.6	−68.9	−9.3	−60.2	−0.6	−62.8	−3.2
4	−73.4	−74.5	−1.1	−80.9	−7.5	−86.0	−12.6	−77.7	−4.3	−80.7	−7.3
5	−85.7	−85.9	−0.2	−92.6	−6.9	−101.7	−16.0	−90.7	−5.0	−94.0	−8.3
6	−96.4	−97.1	−0.7	−104.1	−7.7	−117.8	−21.4	−100.9	−4.5	−105.1	−8.7
mean			−0.2		−5.7		−11.2		−2.1		−5.0
std dev			0.8		2.4		7.0		2.9		3.3

	exptl[b]	EFP/6-31+G*		RHF/6-31+G*		MP2/6-31+G*		MP2/aug-cc-pVDZ		MP2/aug-cc-pVTZ	
$K^+(H_2O)_n$	$\Delta_r H^0$	$\Delta_r H^0$	error	$\Delta_r H^0$	error	$\Delta_r H^0$	error	$\Delta_r H^0$	error	$\Delta_r H^0$	error
1	−17.9	−18.6	−0.7	−18.3	−0.4	−20.1	−2.2				
2	−34.0	−34.3	−0.3	−33.6	0.4	−37.5	−3.5				
3	−47.2	−48.1	−0.9	−47.1	0.1	−51.8	−4.6				
4	−59.0	−59.7	−0.7	−58.2	0.8	−64.5	−5.5				
5	−69.7	−70.9	−1.2	−69.2	0.5	−79.5	−9.8				
6	−79.7	−81.8	−2.1	−80.0	−0.3	−93.0	−13.3				
mean			−1.0		0.2		−6.5				
std dev			0.6		0.4		4.2				

	exptl	EFP/6-31+G*		RHF/6-31+G*		MP2/6-31+G*		MP2/aug-cc-pVDZ		MP2/aug-cc-pVTZ	
$Mg^{2+}(H_2O)_n$	$\Delta_r H^0$	$\Delta_r H^0$	error	$\Delta_r H^0$	error	$\Delta_r H^0$	error	$\Delta_r H^0$	error	$\Delta_r H^0$	error
1		−66.6		−80.1		−81.6		−77.5		−80.5	
2		−127.4		−151.3		−154.3		−146.0		−154.9	
3		−180.0		−209.6		−214.4		−202.1		−211.3	
4		−224.8		−256.9		−264.4		−248.7		−259.1	
5		−260.1		−288.1		−299.3		−282.3		−298.2	
6		−289.0		−316.9		−331.8		−314.0		−341.7	
mean											
std dev											

	exptl	EFP/6-31+G*		RHF/6-31+G*		MP2/6-31+G*		MP2/aug-cc-pVDZ		MP2/aug-cc-pVTZ	
$Ca^{2+}(H_2O)_n$	$\Delta_r H^0$	$\Delta_r H^0$	error	$\Delta_r H^0$	error	$\Delta_r H^0$	error	$\Delta_r H^0$	error	$\Delta_r H^0$	error
1		−52.6		−55.0		−58.0					
2		−99.5		−103.1		−109.3					
3		−141.9		−146.2		−153.9					
4		−179.3		−183.7		−193.7					
5		−210.2		−213.8		−226.6					
6		−238.1		−241.0		−257.2					
mean											
std dev											

[a] MP2/aug-cc-pVTZ values are single-point energies on MP2/aug-cc-pVDZ geometries. See the text for details. [b] Reference 11b. [c] Reference 11a.

the RHF/6-31+G* structures for the $Mg^{2+}(H_2O)_{1-6}$ clusters, showing virtually no average error or standard deviation. For the $Ca^{2+}(H_2O)_{1-6}$ clusters, the MP2/6-31+G* structures lead to a slight shortening of the $Ca^{2+}\cdots O$ distances, similar to that seen in the alkali metal cation/water complexes (MSE = −0.02 Å; σ = 0.01 Å). Benchmark MP2/aug-cc-pVDZ optimizations for the $Mg^{2+}(H_2O)_{1-6}$ clusters closely reproduce structures determined at the RHF/6-31+G* and MP2/6-31+G* levels, leading one to conclude that the RHF/6-31+G* level again yields reasonable structures.

What is chemically interesting about these clusters is how they differ from those discussed in the preceding section. Unlike the alkali metal cation/water complexes, the fifth and sixth water molecules of the alkaline earth cation/water clusters do not go into the second solvation shell but interact directly with the cations (see structures VA and VIA in Figure 1). This is all the more noteworthy when the ionic radii of Li^+ (0.90 Å), Na^+ (1.16 Å), Mg^{2+} (0.86 Å), K^+ (1.52 Å), and Ca^{2+} (1.14 Å) are considered;[24] even though the alkaline earth cations possess smaller ionic radii, they accommodate more water molecules

TABLE 4: Mulliken Charges (*q*), Bond Orders (BO), and Components of Reduced Variational Space (RVS) Analysis for Alkali Metal/Alkaline Earth Cation Water Clusters, $X(H_2O)_{1-6}$, X = Li^+, Na^+, K^+, Mg^{2+}, or Ca^{2+}, Performed at the RHF/6-31+G* Level of Theory[a]

$Li^+(H_2O)_n$	q(M)/q(H_2O)	BO(M···O)	ESEX	POL	CT	BSSE	total	$\Delta_r H^0$ (CP)	error
1	0.87/0.13	0.28	−28.1	−7.3	−0.4	−1.0	−35.8	−34.8	−0.8
2	0.76/0.12	0.24	−54.7	−12.3	0.0	−2.5	−67.0	−64.1	−4.3
3	0.69/0.10	0.20	−77.8	−14.0	0.5	−3.4	−91.3	−86.2	−5.7
4	0.61/0.10	0.19	−96.2	−13.3	1.5	−4.6	−108.0	−101.2	−4.3
5	0.64/0.07	0.17	−106.4	−15.4	0.2	−5.6	−121.6	−112.5	−1.7
6	0.68/0.05	0.16	−116.8	−16.9	−0.7	−6.4	−134.4	−123.2	−0.3
								mean	−2.8
								std dev	2.0

$Na^+(H_2O)_n$	q(M)/q(H_2O)	BO(M···O)	ESEX	POL	CT	BSSE	total	$\Delta_r H^0$ (CP)	error
1	0.99/0.01	0.00	−22.2	−3.8	0.5	−0.7	−25.5	−24.8	−0.8
2	0.99/0.00	0.00	−43.1	−6.6	1.2	−1.5	−48.5	−46.3	−2.5
3	1.02/−0.01	0.00	−61.6	−7.9	1.6	−2.1	−67.9	−64.1	−4.5
4	1.06/−0.02	0.00	−77.3	−8.0	1.8	−2.8	−83.5	−78.1	−4.7
5	1.09/−0.02	0.00	−87.1	−10.0	0.8	−3.8	−96.3	−88.8	−3.1
6	1.11/−0.02	0.00	−96.8	−11.8	−0.2	−4.8	−108.8	−99.3	−2.9
								mean	−3.1
								std dev	1.3

$K^+(H_2O)_n$	q(M)/q(H_2O)	BO (M−O)	ESEX	POL	CT	BSSE	total	$\Delta_r H^0$ (CP)	error
1	0.99/0.01	0.00	−15.9	−2.3	−0.3	−0.3	−18.5	−18.0	−0.1
2	0.99/0.00	0.00	−31.0	−3.7	−0.5	−0.5	−35.2	−33.1	0.9
3	0.99/0.00	0.00	−44.8	−4.5	−0.6	−0.7	−49.9	−46.4	0.8
4	0.99/0.00	0.00	−56.9	−4.8	−0.6	−0.9	−62.3	−57.3	1.7
5	0.99/0.00	0.00	−66.0	−6.8	−1.6	−1.9	−74.4	−67.3	2.4
6	1.00/0.00	0.00	−75.1	−8.5	−2.5	−2.9	−86.1	−77.1	2.6
								mean	1.4
								std dev	0.9

$Mg^{2+}(H_2O)_n$	q(M)/q(H_2O)	BO(M···O)	ESEX	POL	CT	BSSE	total	$\Delta_r H^0$ (CP)	error
1	1.76/0.24	0.45	−52.9	−24.5	−2.9	−0.9	−80.3	−79.2	
2	1.55/0.22	0.41	−104.5	−44.7	−4.7	−2.0	−153.9	−149.3	
3	1.46/0.18	0.33	−152.9	−57.9	−5.2	−3.2	−216.0	−206.4	
4	1.36/0.16	0.30	−197.1	−65.3	−4.4	−4.5	−226.8	−252.4	
5	1.34/0.13	0.25	−232.8	−64.1	−3.4	−6.1	−300.3	−282.0	
6	1.31/0.12	0.21	−266.3	−62.0	−1.9	−7.8	−330.2	−309.1	
								mean	
								std dev	

$Ca^{2+}(H_2O)_n$	q(M)/q(H_2O)	BO(M···O)	ESEX	POL	CT	BSSE	total	$\Delta_r H^0$ (CP)	error
1	1.92/0.08	0.14	−37.2	−13.7	−4.3	−0.5	−55.2	−54.5	
2	1.86/0.07	0.12	−74.2	−24.3	−7.0	−1.1	−105.5	−102.0	
3	1.81/0.06	0.11	−110.0	−32.3	−8.8	−1.6	−151.1	−144.6	
4	1.78/0.06	0.10	−143.8	−37.6	−9.9	−2.0	−191.3	−181.7	
5	1.79/0.04	0.08	−174.7	−39.1	−9.7	−3.0	−223.5	−210.8	
6	1.80/0.03	0.11	−203.8	−39.5	−9.2	−3.8	−252.5	−237.2	
								mean	
								std dev	

[a] q(M) = the charge on the metal; q(H_2O) = the average charge transferred per water molecule; BO(M···O) = the average bond order between the metal and the oxygen atom of the water molecule; total = electrostatic/exchange (ESEX) + polarization (POL) + charge transfer (CT); and CP = counterpoise-corrected. All charges and bond orders are in electrons; all energies are in kcal/mol. See the text for details

in the first hydration shell. This clearly demonstrates the strength of the electrostatic attractions (primarily charge−dipole) relative to the repulsive ligand−ligand interactions between the water molecules (Table 4).

Differential standard enthalpies of hydration (eq 1) for the $Mg^{2+}(H_2O)_{1-6}$ and $Ca^{2+}(H_2O)_{1-6}$ clusters can be found in Table 2. A comparison of the EFP/6-31+G* and RHF/6-31+G* $\Delta\Delta_r H^0$ values for the Mg^{2+} water clusters shows large differences for the smaller clusters with some improvement in agreement for the larger clusters: $\Delta\Delta_r H^0$ (EFP) − $\Delta\Delta_r H^0$ (RHF) = 13.5, 10.4, 5.8, 2.4, −4.0, and −0.1 kcal/mol for one to six water molecules, respectively. The EFP method is clearly not capable of accurately reproducing the RHF results for the smaller $Mg^{2+}(H_2O)_{1-6}$ clusters. Comparison with available experimental data for five and six water molecules suggests that both the EFP/6-31+G* and RHF/6-31+G* levels exhibit overbinding. Introduction of electron correlation at the MP2/6-31+G* level does not reduce this overbinding. Furthermore, the benchmark calculations at the MP2/aug-cc-pVDZ level of theory show only a modest reduction in the overbinding compared with experiment. In contrast to the $Mg^{2+}(H_2O)_{1-6}$ clusters, the EFP/6-31+G* and RHF/6-31+G* $\Delta\Delta_r H^0$ values for the $Ca^{2+}(H_2O)_{1-6}$ clusters show excellent agreement. Comparison with the experimental data for five and six water molecules suggests overbinding at both of these levels of theory. This overbinding increases slightly at the MP2/6-31+G* level of theory. As the experimental $\Delta\Delta_r H^0$ values are estimates based upon a number of assumptions, the uncertainties associated with these measure-

TABLE 5: Mean Errors and Standard Deviations for Total and Differential Internal Energies ($\Delta_r E^0$ and $\Delta\Delta_r E^0$) and Enthalpies ($\Delta_r H^0$ and $\Delta\Delta_r H^0$) of Reaction at 0 K for the Alkali Metal Cation Water Clusters, $X^+(H_2O)_{1-6}$, X = Li, Na, and K[a]

		EFP/6-31+G*		HF/6-31+G*		MP2/6-31+G*	
$X^+(H_2O)_{1-6}$		$\Delta_r E^0$	$\Delta\Delta_r E^0$	$\Delta_r E^0$	$\Delta\Delta_r E^0$	$\Delta_r E^0$	$\Delta\Delta_r E^0$
Li	mean	−10.3	−2.4	−11.8	−2.7	−17.8	−4.8
	std dev	4.8	1.9	5.0	2.3	9.1	1.8
Na	mean	−5.0	−1.7	−10.3	2.8	−15.3	−4.7
	std dev	3.8	1.1	5.3	1.0	9.3	1.0
K	mean	−5.6	−1.9	−4.2	−1.5	−10.4	−3.6
	std dev	3.7	0.8	3.0	0.9	7.0	1.7

		EFP/6-31+G*		HF/6-31+G*		MP2/6-31+G*	
$X^+(H_2O)_{1-6}$		$\Delta_r H^0$	$\Delta\Delta_r H^0$	$\Delta_r H^0$	$\Delta\Delta_r H^0$	$\Delta_r H^0$	$\Delta\Delta_r H^0$
Li	mean	−2.7	−0.1	−4.9	−0.6	−10.9	−2.7
	std dev	2.3	2.4	2.5	2.5	5.4	2.0
Na	mean	0.9	0.3	−4.4	−0.9	−9.5	−2.8
	std dev	0.9	1.2	2.2	1.5	5.7	1.0
K	mean	−0.2	0.0	1.0	0.3	−10.8	−1.8
	std dev	0.3	0.4	0.6	0.4	−5.3	0.8

[a] All values are in kcal/mol.

ments may be somewhat larger than those of the alkali metal cation systems.

Total standard enthalpies of hydration (eq 2) for the $Mg^{2+}(H_2O)_{1-6}$ and $Ca^{2+}(H_2O)_{1-6}$ clusters are listed in Table 3. For the $Mg^{2+}(H_2O)_{1-6}$ clusters, the RHF/6-31+G* level exhibits stronger binding energies than at the EFP/6-31+G* level. The binding energies increase further on going to the MP2/6-31+G* level of theory. The benchmark MP2/aug-cc-pVDZ calculations show a modest reduction in binding energies, demonstrating a definite basis set effect. Unlike the differences for the lithium cation clusters, however, these significant differences between the EFP and ab initio levels cannot be explained mainly as the result of basis set superposition error, as this error averages only 1.1 kcal/mol per water molecule (Table 4). The inclusion of a counterpoise (CP) correction does not, therefore, significantly improve the large differences for the small Mg^{2+} clusters whereas it actually leads to poorer agreement for the larger ones.

For the $Ca^{2+}(H_2O)_{1-6}$ clusters, the EFP/6-31+G* and RHF/6-31+G* total enthalpies of hydration agree quite closely. An increase in binding energy is, once again, seen on going from the RHF/6-31+G* to MP2/6-31+G* level. In addition, Table 4 shows only a very small BSSE at the RHF/6-31+G* level for the $Ca^{2+}(H_2O)_{1-6}$ clusters (0.6 kcal/mol per water molecule).

From the preceding results, it can be concluded that the EFP method is not capable of accurately reproducing the RHF enthalpies of hydration for the $Mg^{2+}(H_2O)_{1-6}$ clusters, but it appears to be quite able to duplicate them for the $Ca^{2+}(H_2O)_{1-6}$ clusters. This seems to be somewhat surprising as both systems are doubly charged, and one might expect the EFP method, originally designed for neutral cases, to break down for both of them. A possible explanation for this different behavior may lie with the varying degrees of charge transfer in the two systems. Table 4 shows the Mulliken charges and average bond orders at the RHF/6-31+G* level of theory for the two systems. On the basis of the Mulliken charges, q(M), an appreciable amount of charge has been transferred from the water molecules to the metal cations in the Mg^{2+} clusters. In addition, the metal−oxygen bond orders, BO(M···O), are suggestive of dative-type bonds between the magnesium and oxygen atoms. For the $Ca^{2+}(H_2O)_{1-6}$ clusters, the Mulliken charges reveal that only a small amount of charge has been transferred from the water molecules to the calcium cations, leading to smaller BO(M···O) values. One is led to conclude that the EFP model cannot properly describe systems with high degrees of charge transfer. As the EFP method's charge-transfer component was derived from a fitting procedure for the water dimer, a system with little charge transfer, it is not too surprising that the model fails in the case of the $Mg^{2+}(H_2O)_{1-6}$ clusters. The EFP method's inability to account adequately for charge transfer may help to explain the long $Mg^{2+}\cdots O$ bonds. Charge transfer leads to the formation of dative-type bonds and thus shorter bond lengths; in the absence of an adequate description of charge transfer, the elongated bonds are understandable.

TABLE 6: Total, $\Delta_r H^0$, and Differential, $\Delta\Delta_r H^0$, Standard Enthalpies of Hydration for the Formation of $Li^+(H_2O)_{1-6}$, $Na^+(H_2O)_{1-6}$, and $Mg^{2+}(H_2O)_{1-6}$ Clusters Computed at the MP2/aug-cc-pVDZ//EFP/6-31+G* Level of Theory (kcal/mol)[a]

	$M + nH_2O \rightarrow M(H_2O)_n$, $n = 1-6$, M = Li^+, Na^+, or Mg^{2+}								
	Li^+			Na^+			Mg^{2+}		
$M(H_2O)_n$	exptl	calcd	error	exptl	calcd	error	exptl	calcd	error
1	−34.0	−33.1	0.9	−24.0	−21.8	2.2		−73.6	
2	−59.8	−63.1	−3.3	−43.8	−40.9	2.9		−139.2	
3	−80.5	−84.7	−4.2	−59.6	−57.2	2.4		−193.6	
4	−96.9	−101.4	−4.5	−73.4	−72.1	1.3		−238.5	
5	−110.8	−113.3	−2.5	−85.7	−84.3	1.4		−272.2	
6	−122.9	−125.1	−2.2	−96.4	−96.2	0.2		−298.0	
mean			−2.6			1.7			
std dev			1.9			1.0			

	$M(H_2O)_{n-1} + H_2O \rightarrow M(H_2O)_n$, $n = 1-6$, M = Li^+, Na^+, or Mg^{2+}								
	Li^+			Na^+			Mg^{2+}		
$M(H_2O)_n$	exptl	calcd	error	exptl	calcd	error	exptl	calcd	error
1	−34.0	−33.1	0.9	−24.0	−21.8	2.2		−73.6	
2	−25.8	−29.9	−4.1	−19.8	−19.0	0.8		−65.6	
3	−20.7	−21.7	−1.0	−15.8	−16.4	−0.6		−54.4	
4	−16.4	−16.7	−0.3	−13.8	−14.8	−1.0		−44.9	
5	−13.9	−11.9	2.0	−12.3	−12.2	0.1	−26.3	−33.7	−7.4
6	−12.1	−11.8	0.3	−10.7	−11.9	−1.2	−24.2	−25.8	−1.6
mean			−0.4			0.0			
std dev			2.1			1.3			

[a] See the text for details.

A second possible source of error may reside with the polarization component of the EFP method. Consider the RVS analyses of the $Li^+(H_2O)_{1-6}$ and $Mg^{2+}(H_2O)_{1-6}$ clusters. As would be expected on going from a singly charged to a doubly charged species, the latter's electrostatic component approximately doubles. The polarization component, however, more than triples in going from the $Li^+(H_2O)_{1-6}$ to the $Mg^{2+}(H_2O)_{1-6}$ clusters. As can be seen in Table 4, the polarization contribution per water molecule decreases with increasing cluster size, and this effect should, therefore, be most important for the smaller clusters. In the present implementation of the EFP scheme, the polarizabilities are truncated at the dipole term. It may well be that inclusion of quadrupole and higher terms would serve to alleviate some of the apparent underbinding seen for the $Mg^{2+}(H_2O)_{1-6}$ clusters.

IV. Conclusions

The effective fragment potential (EFP) method is capable of reproducing the RHF/6-31+G* differential enthalpies of hydration for the alkali metal cations (Li^+, Na^+, and K^+) and one of the alkaline earth cations (Ca^{2+}) by up to six water molecules. However, the EFP method predicts severe underbinding for the magnesium cation systems compared to the RHF/6-31+G* level of theory. The origin of this apparent underbinding may involve the charge transfer and polarization components of the EFP model and is currently being investigated in our laboratory and in those of others.

The differential enthalpies of hydration computed at the EFP/6-31+G* and RHF/6-31+G* levels are in excellent agreement with the experimental data for the alkali metal cation/water clusters. As the EFP water molecules have no basis functions and therefore introduce no basis set superposition errors, the EFP/6-31+G* level is able to reproduce the experimental total enthalpies of hydration for these systems as well. On the basis of the limited experimental data for the alkaline earth cation systems, the EFP results are in fairly good agreement with experiment for the $Ca^{2+}(H_2O)_{5-6}$ clusters.

Although structural agreement between the EFP method and RHF level of theory for the alkali metal/alkaline earth cation water clusters is generally quite good, the EFP structures for the $Na^+(H_2O)_{1-6}$ and $Mg^{2+}(H_2O)_{1-6}$ clusters possess M···O distances that are too long. However, the potential energy surfaces for these cation−water systems are fairly flat: what would be considered large structural differences for covalently bonded structures do not translate into large energetic differences for these more weakly bound complexes. This shortcoming appears to be of minor importance for systems with little or modest charge transfer given that the EFP calculations reproduce the experimental differential and total enthalpies of hydration for the $Na^+(H_2O)_{1-6}$ clusters. Systems that exhibit a significant degree of charge transfer (e.g., $Mg^{2+}(H_2O)_{1-6}$) should be approached with caution when using the EFP model.

Given the MP2/aug-cc-pVDZ results for the $Na^+(H_2O)_{1-6}$ and $Mg^{2+}(H_2O)_{1-6}$ clusters, a model chemistry immediately suggests itself. For cases when the EFP method may be suspect in reproducing enthalpies or the active region of the system requires a correlated wavefunction, the use of MP2/aug-cc-pVDZ single-point energies on EFP/6-31+G* optimized structures and Hessians appears viable. Total and differential enthalpies for the $Li^+(H_2O)_{1-6}$, $Na^+(H_2O)_{1-6}$, and $Mg^{2+}(H_2O)_{1-6}$ clusters[25] calculated with this model are given in Table 6. The model clearly performs very well with most of the values for the $Li^+(H_2O)_{1-6}$ and $Na^+(H_2O)_{1-6}$ clusters falling within the experimental range of uncertainty. Little experimental data is available for the $Mg^{2+}(H_2O)_{1-6}$ clusters.

Notwithstanding systems exhibiting large degrees of charge transfer, the EFP/6-31+G* model appears to offer an inexpensive and accurate approach to the description of solvation in simple cationic systems. It should, therefore, hold great promise in the modeling of larger solvated systems. For example, Netzloff and co-workers[26] have used the effective fragment potential in molecular dynamics (MD) calculations involving up to 256 water molecules and have obtained ab initio quality results.

Acknowledgment. It is a pleasure to acknowledge the assistance of Professor Mark Gordon (Department of Chemistry, Iowa State University), who read and commented upon an earlier draft of this paper; Dr. Mike Schmidt (Department of Chemistry, Iowa State University) for helpful discussions regarding the RVS method; and Professor Paul Kebarle (Department of Chemistry, University of Alberta) for elaboration of his experimental results.

References and Notes

(1) Voet, D.; Voet, J. G. *Biochemistry*, 2nd ed; Wiley and Sons: New York, 1995.

(2) Feller, D. *J. Phys. Chem. A* **1997**, *101*, 2723. This study deals with the alkali metal cations (Li^+, Na^+, K^+, Rb^+, and Cs^+). A related study of the alkaline earth dications (Mg^{2+}, Ca^{2+}, Sr^{2+}, Ba^{2+}, and Ra^{2+}) can be found in Glendening, E. D.; Feller, D. *J. Am. Chem. Soc.* **1996**, *118*, 6052.

(3) Cramer, C. J.; Truhlar, D. G. In *Reviews in Computational Chemistry;* Lipkowitz, K. B., Boyd, D. B., Eds.; VCH: New York, 1995; Vol. 6.

(4) (a) Miertus, S.; Scrocco, E.; Tomasi, J. *Chem. Phys.* **1981**, *55*, 117. (b) Tomasi, J.; Persico, M. *Chem. Rev.* **1994**, *94*, 2027. (c) Cammi, R.; Tomasi, J. *J. Comput. Chem.* **1995**, *16*, 1449.

(5) We know of no general review of the supermolecular approach. The results of this method are scattered over dozens of articles. An example of one such study is Jensen, J. H.; Gordon, M. S. *J. Am. Chem. Soc.* **1995**, *117*, 8159.

(6) Gao, J. In *Reviews in Computational Chemistry;* Lipkowitz, K. B., Boyd, D. B., Eds.; VCH: New York, 1996; Vol. 7.

(7) (a) Jensen, J. H.; Day, P. N.; Gordon, M. S.; Basch, H.; Cohen, D.; Garmer, D. R.; Kraus, M.; Stevens, W. J. In *Modelling the Hydrogen Bond;* Smith, D. A., Ed.; ACS Symposium Series; American Chemical Society: Washington, DC, 1994; Vol. 569. (b) Day, P. N.; Jensen, J. H.; Gordon, M. S.; Webb, S. P.; Stevens, W. J.; Krauss, M.; Garmer, D.; Basch, H.; Cohen, D. *J. Chem. Phys.* **1996**, *105*, 1968.

(8) Restricted Hartree−Fock (RHF) calculations scale approximately as the number of basis functions (N) to the fourth power (i.e., $\sim N^4$) If $N = 168$, then $N^4 = 796\,594\,176$. If $N = 30$, then $N^4 = 810\,000$. The ratio of the latter to the former is, therefore, approximately 0.001 or 0.1%.

(9) Second-order Møller−Plesset (MP2) calculations scale approximately as N,[5] where N is the number of basis functions. Using the example cited in the text, if $N = 168$, then $N^5 = 133\,827\,821\,568$; if $N = 30$, then $N^5 = 24\,300\,000$. The ratio of the latter to the former is approximately 0.0002 or 0.02%.

(10) (a) Chen, W.; Gordon, M. S. *J. Chem. Phys.* **1996**, *105*, 11081. (b) Jensen, J. H.; Gordon, M. S. *J. Chem. Phys.* **1998**, *108*, 4772. (c) Merrill, G. N.; Gordon, M. S. *J. Phys. Chem. A* **1998**, *102*, 2650. (d) Webb, S. P.; Gordon, M. S. *J. Phys. Chem. A* **1999**, *103*, 1265. (e) Gordon, M. S.; Peterson, C. *J. Phys. Chem. A* **1999**, *103*, 4162. (f) Day, P. N.; Pachter, R.; Gordon, M. S.; Merrill, G. N. *J. Chem. Phys.* **2000**, *112*, 2063. (g) Damrauer, R. *J. Am. Chem. Soc.* **2000**, *122*, 6739. (h) Gordon, M. S.; Freitag, M. A.; Bandyopadhyay, P.; Kairys, V.; Jensen, J. H.; Stevens, W. J. *J. Phys. Chem A.* **2001**, *105*, 293.

(11) (a) Searles, S. K.; Kebarle, P. *Can. J. Chem.* **1969**, *47*, 2619. (b) Dzidic, I.; Kebarle, P. *J. Phys. Chem.* **1970**, *74*, 1466. (c) Tang, I. N.; Castleman, A. W., Jr. *J. Chem. Phys.* **1972**, *57*, 3638. (d) Tang, I. N.; Lian, M. S.; Castleman, A. W., Jr. *J. Chem. Phys.* **1976**, *65*, 4022. (e) Burdett, N. A.; Hayhurst, A. N. *J. Chem. Soc., Faraday Trans. 1* **1982**, *78*, 2997. (f) Keese, R. G.; Castleman, A. W. *J. Phys. Chem. Ref. Data* **1986**, *15*, 1011. (g) Blades, A. T.; Jayaweera, P.; Ikonomou, M. G.; Kebarle, P. *J. Chem. Phys.* **1990**, *92*, 5900. (h) Blades, A. T.; Klassen, J. S.; Kebarle, P. *J. Am. Chem. Soc.* **1996**, *118*, 12437. (i) Peschke, M.; Blades, A. T.; Kebarle, P. *J. Phys. Chem. A* **1998**, *102*, 9978. (j) Rodriguez-Cruz, S. E.; Jockusch, R. A.; Williams, E. R. *J. Am. Chem. Soc.* **1999**, *121*, 8898. (k) Schvartsburg, A. A.; Siu, K. W. M. *J. Am. Chem. Soc.* **2001**, *123*, 10071.

(12) (a) Cieplak, P.; Lybrand, T. P.; Kollman, P. A. *J. Phys. Chem.* **1987**, *86*, 6393. (b) Bauschlicher, C. W., Jr.; Langhoff, S. R.; Partridge, H.; Rice, J. E.; Komornicki, A. *J. Chem. Phys.* **1991**, *95*, 5142. (c) Klobukowski, M. *Can. J. Chem.* **1992**, *70*, 589. (d) Bauschlicher, C. W.,

Jr.; Sodupe, M.; Partridge, H. *J. Chem. Phys.* **1992**, *96*, 4453. (e) Feller, D.; Glendening, E. D.; Kendall, R. A.; Peterson, K. A. *J. Chem. Phys.* **1994**, *100*, 4981. (f) Kim, J.; Lee, S.; Cho, S. J.; Mhin, B. J.; Kim, K. S. *J. Chem. Phys.* **1995**, *103*, 839. (g) Feller, D.; Glendening, E. D.; Woon, D. E. *J. Chem. Phys.* **1995**, *103*, 3526. (h) Glendening, E. D.; Feller, D. *J. Phys. Chem.* **1995**, *99*, 3060. Our current results essentially reproduce those of Glendening and Feller with a few minor exceptions; these differences are largely attributable to the use of different counterpoise methods. The counterpoise (CP) correction used by Glendening and Feller is that of Boys and Bernardi (Boys, S. F.; Bernardi, F. *Mol. Phys.* **1970**, *19*, 553.) The current CP correction is due to Cammi et al.[22] Glendening and Feller also use the effective core potential (ECP) of Hay and Wadt (Hay, P. J.; Wadt, W. R. *J. Chem. Phys.* **1985**, *82*, 299) for the potassium atom. At the Hartree−Fock level, they do not report a D_{2d} structure for the $M^+(H_2O)_6$ (M = Li, Na, and K) clusters. These structures appear to be lower in energy then the C_s ($Li^+(H_2O)_6$), C_1 ($Na^+(H_2O)_6$), and D_3 ($K^+(H_2O)_6$) structures. At the second-order Møller−Plesset level, Glendening and Feller freeze the 1s orbital for lithium and the 1s, 2s, and 2p orbitals for sodium. In the current calculations, no orbitals are frozen for lithium, and only the 1s orbital is frozen for sodium, which leads to lower binding enthalpies. (i) Glendening, E. D.; Feller, D. *J. Phys. Chem.* **1996**, *100*, 589. Our current counterpoise-corrected results at the HF/6-31+G* level (Table 4) are in fair agreement with those reported by Glendening and Feller, with a slightly greater degree of binding predicted ($Mg^{2+} = -2.8$; $Ca^{2+} = -2.0$ kcal/mol). These differences can be attributed to the use of different counterpoise (CP) corrections. Glendening and Feller have also carried out a series of MP2/6-31+G* single-point energy calculations on top of the HF/6-31+G*-optimized geometries. Comparisons are more tenuous, as our values are based upon MP2-optimized structures. Our values evince far greater binding, but it should be noted that they do not include a CP correction. Glendening and Feller also report T_h symmetric structures for the $Mg^{2+}(H_2O)_{1-6}$ and $Ca^{2+}(H_2O)_{1-6}$ clusters. (j) Pavlov, M.; Siegbahn, P. E. M.; Sandström, M. *J. Phys. Chem. A* **1998**, *102*, 219. (k) Rempe, S. B.; Pratt, L. R. *Fluid Phase Equilib.* **2001**, *183−184*, 121. (l) Lyubartsev, A. P.; Laasonen, K.; Laaksonen, A. *J. Chem. Phys.* **2001**, *114*, 3120. (m) Derepas, A.-L.; Soudan, J.-M.; Brenner, V.; Dognon, J.-P.; Mille, P. *J. Comput. Chem.* **2002**, *23*, 1013.

(13) Manuscript in preparation.

(14) (a) Hehre, W. J.; Ditchfield, R.; Pople, J. A. *J. Chem. Phys.* **1972**, *56*, 2257. (b) Hariharan, P. C.; Pople, J. A. *Theor. Chim. Acta* **1973**, *28*, 213. (c) Dill, J. D.; Pople, J. A. *J. Chem. Phys.* **1975**, *62*, 2921. (d) Krishnan, R.; Binkley, J. S.; Seeger, R.; Pople, J. A. *J. Chem. Phys.* **1980**, *72*, 650. (e) McLean, A. D.; Chandler, G. S. *J. Chem. Phys.* **1980**, *72*, 5639. (f) Francl, M. M.; Petro, W. J.; Hehre, W. J.; Binkley, J. S.; Gordon, M. S.; DeFrees, D. J.; Pople, J. A. *J. Chem. Phys.* **1982**, *77*, 3654. (g) Clark, T.; Chandrasekhar, J.; Schleyer, P. V. R. *J. Comput. Chem.* **1983**, *4*, 294. (h) Blaudeau, J.-P.; McGrath, M. P.; Curtiss, L. A.; Radom, L. *J. Chem. Phys.* **1997**, *107*, 5016. (i) Rassolov, V.; Pople, J. A.; Ratner, M.; Windus, T. L. *J. Chem. Phys.* **1998**, *109*, 1223.

(15) Fletcher, G. D.; Rendell, A. P.; Sherwood, P. *Mol. Phys.* **1997**, *91*, 431.

(16) Scott, A. P.; Radom, L. *J. Phys. Chem.* **1996**, *100*, 16502.

(17) (a) Dunning, T. H., Jr. *J. Chem. Phys.* **1989**, *90*, 1007. (b) Kendall, R. A.; Dunning, T. H., Jr.; Harrison, R. J. *J. Chem. Phys.* **1992**, *96*, 6769. (c) Na and Mg basis sets: Woon, D. E.; Dunning, T. H., Jr. To be submitted for publication.

(18) Schmidt, M. W.; Baldridge, K. K.; Boatz, J. A.; Elbert, S. T.; Gordon, M. S.; Jensen, J. H.; Koseki, S.; Matsuhaga, N.; Nguyen, K. A.; Su, S. J.; Windus, T. L.; Dupuis, M.; Montgomery, J. A. *J. Comput. Chem.* **1993**, *14*, 1347.

(19) The experimental uncertainty associated with the differential enthalpies of hydration for the alkali metal cations is ±1.0 to 2.0 kcal/mol; Kebarle, P. Personal communication. As the total enthalpies of hydration are derived from these values, the following uncertainties are applicable: $n = 1$, ±1.0 to 2.0 kcal/mol; $n = 2$, ±1.4 to 2.8 kcal/mol; $n = 3$, ±1.7 to 3.5 kcal/mol; $n = 4$, ±2.0 to 4.0 kcal/mol; $n = 5$, ±2.2 to 4.5 kcal/mol; and $n = 6$, ±2.4 to 4.9 kcal/mol.

(20) Glendening, E. D. *J. Am. Chem. Soc.* **1996**, *118*, 2473.

(21) (a) Stevens, W. J.; Fink, W. H. *Chem. Phys. Lett.* **1987**, *139*, 15. (b) Chen, W.; Gordon, M. S. *J. Phys. Chem.* **1996**, *100*, 14316.

(22) Cammi, R.; Bonaccorsi, R.; Tomasi, J. *Theor. Chim. Acta* **1985**, *68*, 271.

(23) (a) Mulliken, R. S. *J. Chem. Phys.* **1955**, *23*, 1833. (b) Mulliken, R. S. *J. Chem. Phys.* **1955**, *23*, 1841.

(24) Huheey, J. E.; Keitner, E. A.; Keitner, R. L. *Inorganic Chemistry*, 4th ed; HarperCollins: New York, 1993.

(25) This model was not applied to the $K^+(H_2O)_{1-6}$ and $Ca^{2+}(H_2O)_{1-6}$ clusters as no Dunning-type basis sets exist for the K and Ca atoms.

(26) Netzloff, H. Personal communication.